

Electrostatic potential in a superconductor

Pavel Lipavský and Jan Koláček

Institute of Physics, Academy of Sciences, Cukrovarnická 10, 16253 Praha 6, Czech Republic

Klaus Morawetz

Max-Planck-Institute for the Physics of Complex Systems, Noethnitzer Str. 38, 01187 Dresden, Germany

Ernst Helmut Brandt

Max-Planck-Institut für Metallforschung, D-70506 Stuttgart, Germany

The electrostatic potential in a superconductor is studied. To this end Bardeen's extension of the Ginzburg-Landau theory to low temperatures is used to derive three Ginzburg-Landau equations – the Maxwell equation for the vector potential, the Schrödinger equation for the wave function and the Poisson equation for the electrostatic potential. The electrostatic and the thermodynamic potential compensate each other to a great extent resulting into an effective potential acting on the superconducting condensate. For the Abrikosov vortex lattice in Niobium, numerical solutions are presented and the different contributions to the electrostatic potential and the related charge distribution are discussed.

I. INTRODUCTION

Even in equilibrium, any inhomogeneous conductor has internal electric fields which keep its charge distribution close to local neutrality. The superconductor is not an exception. While the electrochemical potential is constant, the local chemical potential varies in general with any gradient in the system. A distinct property of the superconductor is that in equilibrium there can be an inhomogeneity due to the diamagnetic electric current.

The electric field in a superconductor with a stationary current has been discussed already in 1937 by Bopp¹. From the hydrodynamic description of a charged liquid, Bopp has concluded that the inertial and Lorentz force created by the current are balanced by the Coulomb force. The corresponding electrostatic potential has the form of a Bernoulli potential².

If the Lorentz force dominates, the Bernoulli potential can also be considered as Hall effect. While it was clear that there has to be a Hall voltage which passes the Lorentz force from electrons to the lattice, its measurements by contacts in standard Hall setups did not show any. It was understood³ that by contacts one observes differences in the electrochemical (not electrostatic) potential but this potential is constant in equilibrium.

With the aim to distinguish the electrostatic potential from the electrochemical one, as late as 1968, Bok and Klein⁴ have used the Kelvin capacitive coupling proposed by Hunt³ and have observed first the Bernoulli potential on the surface of a superconductor. Similar measurements have been performed by Brown and Morris^{5,6} or more recently by Chiang and Shevchenko^{7,8}.

Even a perfect surface establishes itself a very strong defect which essentially modifies the electric field.⁹ It is desirable to observe the internal electric field directly in the bulk of a superconductor. A new experiment in this direction has been performed recently by Kumagai

*et al*¹⁰ who have measured the electric field in a type-II superconductor in mixed state by nuclear quadrupole resonance.

Another consequence of the electric field in the bulk is a charge of the vortex core. Blatter *et al*¹¹ have proposed an experiment by which the vortex charge can be accessed. Such measurement, however, is still to be performed. It is also speculated that the vortex charge affects the motion of vortices and thus plays a role in the sign reversal of the Hall regime¹². Since the theory of the anomalous Hall voltage is still open, one cannot conclude about the core charge from this effect.

In this paper we derive a phenomenological theory of the Ginzburg-Landau (GL) type which allows one to evaluate the electric field in the bulk of superconductors at low temperatures. A brief presentation of this theory has been already published in Ref. 13. Here we present details and show how to handle numerically this theory for the Abrikosov lattice of vortices. The electrostatic potential in the vortex lattice is shown for a selected temperature and the contribution of the electric field to forces acting on the condensate is discussed. Throughout the paper we use the language of the two-fluid model. The fluid of superconducting electrons is called condensate while electrons mean normal electrons.

In the next section we review theoretical approaches to the electric field. In Sec. III A we introduce the free energy which includes the condensation energy of Gorter and Casimir, the kinetic energy of Ginzburg and Landau, and the standard electromagnetic energy. Sec. III B presents the essential part of our approach. We use the variational principle to derive three GL equations: the Maxwell equation for the magnetic field, the Schrödinger equation for the wave function, and the Poisson equation for the electrostatic potential in the bulk of superconductors. In Sec. IV, the hydrodynamic picture is used to link the presented theory with the former approaches

reviewed in Sec. II. In Sec. V we discuss magnetic properties of the Abrikosov vortex lattice as a function of the temperature. In Sec. VI we compare the electrostatic potential with other potentials acting on the condensate. We also present the charge distribution and show that its amplitude is very small what allows one to employ a convenient quasi-neutral approximation. Sec. VII presents the conclusions. In Appendix A we estimate the material parameters for Niobium using the McMillan formula and empirical rules established from chemical trends.

II. HISTORICAL REVIEW

The electric field in superconductors has been studied since the discovery of superconductivity. Accordingly, various approaches to this problem can be found in the literature. We will briefly remind the progress in this field made mainly in late 1960's and early 1970's.

A. Bernoulli potential

The Bernoulli potential for superconductors has been first derived by Bopp¹. Here we follow the later approach of London². The condensate has to obey two equations of motion. First, it is the London condition,

$$m\mathbf{v} = -e\mathbf{A}, \quad (1)$$

where \mathbf{v} is the local velocity of the condensate and \mathbf{A} is the vector potential. Second, it is the Newton equation

$$m\dot{\mathbf{v}} = e(\mathbf{E} + \mathbf{v} \times \mathbf{B}) + \mathbf{F}_s, \quad (2)$$

where the first term is the Lorentz force with the electric field, $\mathbf{E} = -\partial\mathbf{A}/\partial t - \nabla\varphi$, and the magnetic field, $\mathbf{B} = \nabla \times \mathbf{A}$. The additional force \mathbf{F}_s has been treated by different authors within rather different approximations.

Since the motion of the condensate is fully determined by the London condition, one can use the Newton equation to determine the force acting on the condensate. Once the additional force will be specified, this procedure allows one to identify the electrostatic potential φ .

1. Time derivative of the London condition

To bring the London condition into a form which can be easily compared with the Newton equation, we take the total time derivative, $d/dt = \partial/\partial t + (\mathbf{v}\nabla)$, of the London condition (1),

$$m\dot{\mathbf{v}} = -e\frac{\partial\mathbf{A}}{\partial t} - e(\mathbf{v}\nabla)\mathbf{A}. \quad (3)$$

The first term we express via the electric field, $-\partial\mathbf{A}/\partial t = \mathbf{E} + \nabla\varphi$. For the second term we use a vector identity which in components reads

$$\mathbf{v}_j \nabla_j \mathbf{A}_i = -[\mathbf{v} \times \nabla \times \mathbf{A}]_i + \mathbf{v}_j \nabla_i \mathbf{A}_j. \quad (4)$$

In the first term of (4) one can recognize the Lorentz force, $e\mathbf{v} \times \nabla \times \mathbf{A} = e\mathbf{v} \times \mathbf{B}$. In the second term of (4) we substitute \mathbf{A} by the velocity from the London condition, $e\mathbf{v}_j \nabla_i \mathbf{A}_j = -m\mathbf{v}_j \nabla_i \mathbf{v}_j = -\nabla_i \frac{1}{2}mv^2$.

The time derivative of the London condition then reads

$$m\dot{\mathbf{v}} = e(\mathbf{E} + \mathbf{v} \times \mathbf{B}) + \nabla \left(e\varphi + \frac{1}{2}mv^2 \right). \quad (5)$$

This equation can be compared with the Newton equation (2) giving the electrostatic potential as

$$\nabla e\varphi = \mathbf{F}_s - \nabla \frac{1}{2}mv^2. \quad (6)$$

2. Bernoulli potential

London assumed that the motion of the condensate is controlled by the Lorentz force only. In this approximation, there is no additional force,

$$\mathbf{F}_s = 0. \quad (7)$$

From (6) thus follows the electrostatic potential of the Bernoulli type,

$$e\varphi = -\frac{1}{2}mv^2. \quad (8)$$

3. Quasiparticle screening

In 1964 van Vijfeijken and Staas¹⁴ have extended the Bernoulli potential to finite temperatures using the two fluid model. When flowing, normal electrons dissipate energy. Therefore, in the stationary case they have to stay at rest in spite of the presence of an electric field. These authors have introduced an unspecified force,

$$\mathbf{F}_n = e\nabla\varphi, \quad (9)$$

acting on electrons to keep them at rest, $\mathbf{F}_n + e\mathbf{E} = 0$. This force is assumed to result from the interaction between the electrons and the condensate. Accordingly, there has to be a reaction force \mathbf{F}_s acting on the condensate so that the Newton law of action and reaction is fulfilled,

$$n_n \mathbf{F}_n + n_s \mathbf{F}_s = 0, \quad (10)$$

where n_n and n_s are densities of electrons and condensate. From (9) and (10) one finds the additional force,

$$\mathbf{F}_s = -\frac{n_n}{n_s} e\nabla\varphi, \quad (11)$$

and from (6) follows the electrostatic potential

$$e\varphi = -\frac{n_s}{n}\frac{1}{2}mv^2. \quad (12)$$

This is the Bernoulli potential (8) reduced by the share of the condensate on the total density, $n = n_n + n_s$.

The reduction of the Bernoulli potential has become known as “screening by normal electrons” or “quasiparticle screening”. The quasiparticle screening, however, has to be distinguished from the Thomas-Fermi screening present in all metals including superconductors.

4. Thomas-Fermi screening

In superconductors, the screening is the same as in normal metals. Starting from the time-dependent Ginzburg-Landau theory, Jakeman and Pike¹⁵ have derived the Poisson equation for the electric field with the reduced Bernoulli potential as the driving term,

$$e\varphi - \lambda_{TF}^2 \nabla^2 e\varphi = -\frac{n_s}{n}\frac{1}{2}mv^2. \quad (13)$$

Currents change typically on the scale of the London penetration depth or the GL coherence length, which are much larger than the Thomas-Fermi screening length λ_{TF} . The electrostatic potential φ thus can be treated in the limit of strong screening, $\lambda_{TF} \rightarrow 0$, and from (13) one recovers (12).

5. Thermodynamic potential

Already in 1949 Sorokin¹⁶ has followed the hydrodynamic approach of Bopp assuming an unspecified free energy,

$$\mathcal{F}_s = \int d\mathbf{r} f_s, \quad (14)$$

responsible for the superconducting transition. Here f_s is the density of free energy and $d\mathbf{r}$ denotes integration over the sample volume. The free energy leads to a thermodynamic potential,

$$w_s = \frac{\delta \mathcal{F}_s}{\delta n_s} = \frac{\partial f_s}{\partial n_s}, \quad (15)$$

which yields the additional force

$$\mathbf{F}_s = -\nabla w_s. \quad (16)$$

According to (6) the Bernoulli potential is modified as

$$e\varphi = -\frac{1}{2}mv^2 - w_s. \quad (17)$$

The quasiparticle screening is one of the contributions that result from the thermodynamic potential. There are

also other contributions which can provide information about the pairing mechanism.

Unfortunately, London has disregarded the thermodynamic potential in his book² as unknown and unimportant. His objection was correct at that time since the first reliable thermodynamic potential has been derived eight years later by Bardeen, Cooper and Schrieffer¹⁷. On the other hand, the two-fluid free energy of Gorter and Casimir^{18–20} known from 1934, could be used within Sorokin’s approach to provide at least qualitative results. Our approach follows Sorokin, except that we use an explicit thermodynamic potential of Gorter and Casimir and a non-local kinetic energy.

6. Non-local corrections

As shown in Ref. 21, London’s approach can be modified towards strongly inhomogeneous systems using the Schrödinger equation for a Cooper pair,

$$\frac{1}{2m^*} (-i\hbar\nabla - e^*\mathbf{A})^2 \psi + e^*\varphi\psi + 2w_s\psi = 0, \quad (18)$$

instead of the Newton equation (2). Here we have also included the thermodynamic potential w_s neglected in Ref. 21.

From (18) follows directly a quantum modification of the Bernoulli potential,

$$e^*\varphi = -\frac{1}{\psi}\frac{1}{2m^*}(-i\hbar\nabla - e^*\mathbf{A})^2\psi - 2w_s. \quad (19)$$

In the quasi-classical approximation, $(-i\hbar\nabla - e^*\mathbf{A})\psi = m^*\mathbf{v}\psi$, this formula reduces to potential (17) derived by Sorokin.

To obtain the actual value of the potential, the wave function ψ is identified with the GL wave function and solved from the GL equation. Accordingly, the Cooperon mass and charge, $m^* = 2m$ and $e^* = 2e$, appear in the Schrödinger equation (18).

B. Thermodynamic correction

Rickayzen²² proposed a thermodynamic approach to the electric field. He assumes a quadratic dependence of the free energy on the velocity, what limits his study to weak currents. For systems with a parabolic band, the increase of the free energy due to the current equals the kinetic energy of the condensate,

$$f_{\text{kin}} = n_s \frac{1}{2}mv^2. \quad (20)$$

The electrochemical potential, $\nu = E_F + \nu_{\text{kin}} + e\varphi$, is constant in the whole system, therefore $e\varphi = -\nu_{\text{kin}}$. Since $\nu = \partial f / \partial n$, the velocity variation of the local chemical potential is $\nu_{\text{kin}} = \partial f_{\text{kin}} / \partial n$. Accordingly, the electrostatic potential induced by the current reads²²

$$e\varphi = -\frac{\partial n_s}{\partial n} \frac{1}{2} m v^2. \quad (21)$$

Expression (21) generalizes (12). From the phenomenological density of the condensate,

$$n_s = n \left(1 - \frac{T^4}{T_c^4} \right), \quad (22)$$

follows

$$e\varphi = -\frac{n_s}{n} \frac{1}{2} m v^2 + 4 \frac{n_n}{n} \frac{\partial \ln T_c}{\partial \ln n} \frac{1}{2} m v^2. \quad (23)$$

The first term is the reduced Bernoulli potential (12), the second is a thermodynamic correction. According to (22), the first term of (23) depends on the temperature as $1 - T^4/T_c^4$ while the second one goes as T^4/T_c^4 . At higher temperatures the second term dominates.

1. BCS estimate

The density dependence of T_c reflects the pairing mechanism. Its magnitude can be estimated from the BCS relation¹⁷,

$$k_B T_c = 1.14 \hbar \omega_D e^{-\frac{1}{2D}}, \quad (24)$$

where \mathcal{D} is the single-spin density of states, ω_D is the cut-off frequency usually approximated by the Debye temperature, $\hbar \omega_D \approx k_B \theta_D$, and V is the BCS interaction. Assuming that θ_D and V do not depend on the density, one finds

$$\frac{\partial \ln T_c}{\partial \ln n} = \frac{\partial \mathcal{D}}{\partial \ln n} \frac{1}{\mathcal{D}^2 V} \approx -\frac{\partial \ln \mathcal{D}}{\partial \ln n} \ln \frac{\theta_D}{T_c}. \quad (25)$$

It remains to estimate the derivative of the density of states. For systems with a parabolic band the density of states is proportional to the Fermi momentum, $\ln \mathcal{D} \propto k_F$, while the density of electrons is $n \propto k_F^3$. Accordingly, $\partial \ln \mathcal{D} / \partial \ln n \approx 1/3$. For Niobium we have a very similar value $\partial \ln \mathcal{D} / \partial \ln n = 0.32$, see Tab. 1 in Appendix A.

With the BCS estimate (25), the electrostatic potential (23) reads

$$e\varphi = -\frac{1}{2} m v^2 \left(\frac{n_s}{n} + \frac{n_n}{n} \frac{4}{3} \ln \frac{\theta_D}{T_c} \right). \quad (26)$$

For conventional superconductors, θ_D/T_c is of the order of few tens, therefore the thermodynamic correction is the dominant contribution for approximately $T > \frac{2}{3} T_c$.

For Niobium the BCS formula (26) overestimates the thermodynamic correction. The approximate factor from (26) is $(4/3) \ln(\theta_D/T_c) = 4.5$ while the full factor from (23) gives $-4(\partial \ln T_c / \partial \ln n) = 3.0$, see (69) and Appendix A.

2. BCS microscopic theory

Within the BCS theory, the electric field has been studied by Adkins and Waldram²³, Rickayzen²² and Hong²⁴. In all these studies, materials with a general band structure have been addressed. For the sake of simplicity we discuss only the parabolic band, for which the BCS theory yields^{23,24}

$$e\varphi \approx \frac{\Delta^2}{2} \frac{\partial \ln \mathcal{D}}{\partial E_F} \ln \left(\frac{2\omega_D \hbar}{\Delta_0} \right). \quad (27)$$

Here $\Delta_0 = 1.75 k_B T_c$ is the gap at $T = 0$ and Δ is the actual local value of the gap.

Since the electric current locally depresses the gap, $\Delta = \Delta_{\text{eq}} + \Delta'$ with $\Delta' \propto -v^2$, the potential (27) includes the contribution of Bernoulli type, $\varphi = \varphi_{\text{eq}} + \varphi'$ with $\varphi' \propto -v^2$. As shown by Rickayzen²², φ' can be rearranged into the thermodynamic correction of (26).

C. Aims of the present approach

In this paper we discuss the Ginzburg-Landau theory modified in two directions. First, following Bardeen we use its extension to low temperatures. Second, we include the electrostatic potential. We focus on the bulk of superconductors, i.e., on regions which are far from the surface on the scale of Thomas-Fermi screening length.

Starting from the free energy, we derive the Poisson equation along with the Maxwell equation for the vector potential and the equation of the Schrödinger type for the wave function. The presented theory yields

- non-local Bernoulli potential,
- quasiparticle screening,
- thermodynamic corrections,
- thermoelectric field of normal metal at $T = T_c$,
- Thomas-Fermi screening.

Our approach parallels the original study of Sorokin, however, we use the explicit phenomenological free energy proposed by Bardeen. It combines the Ginzburg-Landau (GL) theory with the Gorter-Casimir free energy. Naturally, this theory is only approximate. Its major advantage is its transparency and a simple implementation scheme.

III. EXTENDED GINZBURG-LANDAU THEORY

A. Free energy

Bardeen^{25,26} has extended the GL theory^{27,28} by the use of the Gorter-Casimir two-fluid model¹⁸⁻²⁰ so as to

apply to all temperatures. We briefly recall the Gorter-Casimir model and introduce other components of the free energy.

1. Condensation energy of two-fluid model

Gorter and Casimir assumed that the superconducting state is characterized by an order parameter ϖ which is zero in the normal state and unity at zero temperature. They have modified the normal state density of free energy as

$$f_s = U - \varepsilon_{\text{con}}\varpi - \frac{1}{2}\gamma T^2\sqrt{1-\varpi}. \quad (28)$$

For $\varpi = 0$, the free energy (28) equals the normal state free energy consisting of the internal energy U and the entropy term $-\frac{1}{2}\gamma T^2$. Sommerfeld's γ is the linear coefficient of the specific heat. In the superconducting state, $\varpi \neq 0$, two mechanisms are expected. First, the ordering releases the condensation energy $\varepsilon_{\text{con}}\varpi$. Second, the ordering reduces the entropy by the factor $\sqrt{1-\varpi}$.

In equilibrium the free energy reaches its minimum. From $\delta\mathcal{F}_s/\delta\varpi = \partial f_s/\partial\varpi = 0$ follows that the equilibrium value of the order parameter is a solution of

$$\varepsilon_{\text{con}} = \frac{\gamma T^2}{4\sqrt{1-\varpi}}. \quad (29)$$

At the critical temperature the ordering vanishes, $\varpi = 0$, therefore

$$\varepsilon_{\text{con}} = \frac{1}{4}\gamma T_c^2. \quad (30)$$

From (29) with (30) follows

$$\varpi = 1 - \frac{T^4}{T_c^4}, \quad (31)$$

which agrees with the observed temperature dependence of the condensate density (22). Accordingly, one can identify the order parameter ϖ with the fraction of the condensate on the total density of electrons,

$$\varpi = \frac{n_s}{n}. \quad (32)$$

2. Kinetic energy

An electric current contributes to the free energy by the kinetic energy of the condensate. The kinetic energy proposed by Ginzburg and Landau^{27,28} reads

$$\mathcal{F}_{\text{kin}} = \int d\mathbf{r} \frac{1}{2m^*} |(-i\hbar\nabla - e^*\mathbf{A})\psi|^2, \quad (33)$$

with the wave function normalized as

$$|\psi|^2 = \frac{n_s}{2}. \quad (34)$$

We use the isotropic effective mass for simplicity, the anisotropic case will be discussed in the next paper.

In the Gorter-Casimir free energy we thus substitute the order parameter by

$$\varpi = \frac{2|\psi|^2}{n} = \frac{2|\psi|^2}{2|\psi|^2 + n_n}. \quad (35)$$

3. Electromagnetic energy

The density of free energy has four components,

$$\mathcal{F} = \mathcal{F}_s + \mathcal{F}_{\text{kin}} + \mathcal{F}_C + \mathcal{F}_M. \quad (36)$$

The free energy \mathcal{F}_s given by the volume integral (14) of the free energy density (28), we shall call the condensation energy according to its most important part. The kinetic energy, \mathcal{F}_{kin} , is given by the GL expression (33). The Coulomb interaction reads

$$\mathcal{F}_C = \frac{1}{2} \iint d\mathbf{r} d\mathbf{r}' \frac{1}{4\pi\epsilon} \frac{1}{|\mathbf{r} - \mathbf{r}'|} \rho(\mathbf{r})\rho(\mathbf{r}'), \quad (37)$$

where $\rho = e^*|\psi|^2 + en_n + \rho_{\text{latt}}$ is the charge density. The Coulomb interaction also determines the electrostatic potential, by

$$\varphi(\mathbf{r}) = \int d\mathbf{r}' \frac{1}{4\pi\epsilon} \frac{1}{|\mathbf{r} - \mathbf{r}'|} \rho(\mathbf{r}') \quad (38)$$

or in its differential form by the Poisson equation

$$-\epsilon\nabla^2\varphi = \rho. \quad (39)$$

Finally, the Helmholtz magnetic free energy reads²⁹,

$$\mathcal{F}_M = \int d\mathbf{r} \frac{1}{2\mu_0} (\mathbf{B} - \mathbf{B}_a)^2, \quad (40)$$

where \mathbf{B}_a is the applied magnetic field.

The total free energy is a functional of the wave function, the vector potential and the (normal) electron density, $\mathcal{F}[\psi, \mathbf{A}, n_n]$. The other physical quantities like \mathbf{B} , φ , n , n_s , ρ or ϖ are subsidiary and have to be understood as functions of the independent variables ψ , \mathbf{A} and n_n .

We note that much more sophisticated approximations of the free energy $\mathcal{F}_s + \mathcal{F}_{\text{kin}}$ have been developed from the BCS theory and Eliashberg's theory already in 1960's, see e.g. Ref. 30. In principle, one can start from any of these approximations. Since our prime interest is in the electrostatic potential and the related charge distribution, we prefer to use the simple approximation of Bardeen.

B. Ginzburg-Landau equations of motions

In equilibrium, the system stays in the state with minimum free energy. Accordingly, the variations of \mathcal{F} with respect to the vector potential \mathbf{A} , the wave function ψ and the electron density n_n have to vanish.

During the variation procedure, the two-point function \mathcal{F}_C and the one-point functions (all the others) are treated differently. The local contributions are given by the corresponding densities, $f_\alpha[l(r), \nabla l(r)]$, with $\mathcal{F}_\alpha = \int d\mathbf{r} f_\alpha$, and their variation is of Lagrange's form³¹,

$$\frac{\delta \mathcal{F}_\alpha}{\delta l} = \frac{\partial f_\alpha}{\partial l} - \nabla \frac{\partial f_\alpha}{\partial \nabla l}. \quad (41)$$

Here α represents the subscripts s , kin and M while l stands for \mathbf{A} , ψ or n_n .

The variation of the Coulomb energy with respect to ψ or n_n can be expressed by the variation with respect to the density of charge ρ which reads

$$\frac{\delta \mathcal{F}_C}{\delta \rho(\mathbf{r})} = \int d\mathbf{r}' \frac{1}{4\pi\epsilon} \frac{1}{|\mathbf{r} - \mathbf{r}'|} \rho(\mathbf{r}'). \quad (42)$$

According to (38) we can abbreviate this variation as

$$\frac{\delta \mathcal{F}_C}{\delta \rho} = \varphi. \quad (43)$$

1. Maxwell equation

The vector potential \mathbf{A} appears in the kinetic energy \mathcal{F}_{kin} , and its gradients enter the magnetic free energy via $\mathbf{B} = \nabla \times \mathbf{A}$. From the condition of minimum with respect to \mathbf{A} , one recovers the Maxwell equation,

$$\nabla \times \nabla \times \mathbf{A} = \mu_0 \mathbf{j}, \quad (44)$$

where the current \mathbf{j} is given by the quantum-mechanical formula²⁸,

$$\mathbf{j} = \frac{e^*}{m^*} \text{Re} \bar{\psi} (-i\hbar \nabla - e^* \mathbf{A}) \psi, \quad (45)$$

known as the second GL equation. Here $\bar{\psi}$ denotes the complex conjugate of ψ .

2. Schrödinger equation

The wave function ψ enters the free energy via the order parameter, the Coulomb interaction via the charge density, and the kinetic energy \mathcal{F}_{kin} , where also the gradients of ψ appear. The variation parallels the derivation of the first GL equation²⁸, for details see Ref. 29.

The variation with respect to $\bar{\psi}$ leads to the equation of the Schrödinger type,^{*}

$$\frac{1}{2m^*} (-i\hbar \nabla - e^* \mathbf{A})^2 \psi + \chi \psi = 0. \quad (46)$$

The effective potential,

$$\chi = \frac{\delta}{\delta |\psi|^2} (\mathcal{F}_C + \mathcal{F}_s) = e^* \varphi + \frac{\partial f_s}{\partial |\psi|^2}, \quad (47)$$

covers all forces acting on Cooper pairs.

3. Diffusion of normal electrons

From the variation with respect to the electron density, $\delta \mathcal{F} / \delta n_n = 0$, one finds that the sum of all potentials acting on the normal electrons has to vanish, i.e.,

$$e\varphi = -\frac{\delta \mathcal{F}_s}{\delta n_n} = -\frac{\partial f_s}{\partial n_n}. \quad (48)$$

This condition parallels Eq. (9) of van Vijfeijken and Staas.

The set of equations (44-48) is closed. Its particular form is given by the condensation energy f_s . Below we evaluate derivatives of the condensation energy within the Gorter-Casimir approximation (28).

4. Effective potential acting on Cooper pairs

To describe the motion of the condensate given by the effective potential χ , we have to evaluate the electrostatic potential. This will be done in the spirit of van Vijfeijken and Staas using the equation for normal electrons (48).

Since $e^* = 2e$, the effective potential results from (48) and (47) as

$$\chi = \frac{\partial f_s}{\partial |\psi|^2} - 2 \frac{\partial f_s}{\partial n_n}. \quad (49)$$

The combination of the partial derivatives excludes a contribution of functions which depend exclusively on the total density, $\partial n / \partial |\psi|^2 - 2 \partial n / \partial n_n = 0$. Accordingly, derivatives of density-dependent material parameters (U , ε_{con} , γ and T_c) do not contribute to the potential χ . From (49) and (28) thus follows

* The free energy is a real function which depends on the complex function ψ and its conjugate $\bar{\psi}$. We express absolute values as products, $|\psi|^2 = \bar{\psi}\psi$, and take $\delta\psi$ and $\delta\bar{\psi}$ as independent perturbations, $\delta\mathcal{F} = (\delta\mathcal{F}/\delta\bar{\psi})\delta\bar{\psi} + (\delta\mathcal{F}/\delta\psi)\delta\psi$. Since $\delta\mathcal{F}/\delta\bar{\psi} = \overline{\delta\mathcal{F}/\delta\psi}$, both variations vanish at the same time. The variational condition $\delta\mathcal{F}/\delta\bar{\psi} = 0$ yields the Schrödinger equation.

$$\chi = -2\frac{\varepsilon_{\text{con}}}{n} + \frac{\gamma T^2}{2n} \frac{1}{\sqrt{1 - \frac{2|\psi|^2}{n}}}. \quad (50)$$

With the potential (50), the Schrödinger equation (46) is identical to the extended GL equation proposed by Bardeen^{25,26}.

Close to T_c , the potential χ approaches the quadratic form of Ginzburg and Landau,

$$\chi \rightarrow \alpha + \beta|\psi|^2, \quad (51)$$

with

$$\alpha = \frac{\gamma T_c}{n}(T - T_c), \quad \beta = \frac{\gamma T_c^2}{2n^2}. \quad (52)$$

We note that the effective potential χ depends on the density n via γ and T_c . In principle, one has to iterate the GL equation together with relations for the density n . In practice, deviations of the density from its crystal value are very small, $|n + \rho_{\text{latt}}/e| \ll n$, and the approximation $en \approx -\rho_{\text{latt}}$ is well justified when one solves for ψ and \mathbf{A} .

5. Poisson equation with screening

Now we rearrange (48) into the form of the Poisson equation with the Thomas-Fermi screening. The variation of the free energy in (48) reads

$$\frac{\partial f_s}{\partial n_n} = \frac{\partial U}{\partial n} - \frac{\partial}{\partial n_n} \left(\varepsilon_{\text{con}} \varpi + \frac{1}{2} \gamma T^2 \sqrt{1 - \varpi} \right). \quad (53)$$

The derivative of the internal energy,

$$\frac{\partial U}{\partial n} = E_F, \quad (54)$$

is the Fermi energy at the normal ground state of total electron density n . In the presence of the electrostatic potential, the density n differs from its crystal value, $n_0 = -\rho_{\text{latt}}/e$, by the density perturbation ρ/e . The Fermi energy thus depends on the charge density as

$$E_F = E_F^0 + \frac{\partial E_F}{\partial n} \frac{\rho}{e}, \quad (55)$$

where E_F^0 is the crystal value. As usual in the theory of superconductivity, we associate the crystal Fermi energy with the origin of the energy scale, $E_F^0 = 0$.

The density dependence of the local Fermi energy determines the screening. The density derivative of the Fermi energy is the inverse density of states,

$$\frac{\partial E_F}{\partial n} = \frac{1}{2\mathcal{D}}. \quad (56)$$

Using the Poisson equation (39) to evaluate the charge from the electrostatic potential, $\rho = -\epsilon \nabla^2 \varphi$, one can express the Fermi energy as

$$E_F = -\lambda_{TF}^2 \nabla^2 e\varphi. \quad (57)$$

with the Thomas-Fermi screening length $\lambda_{TF}^2 = \epsilon/(2\mathcal{D}e^2)$.

By a substitution of the Fermi energy (57) in the stability condition for normal electrons (48), we arrive at the screened Poisson equation,

$$e\varphi - \lambda_{TF}^2 \nabla^2 e\varphi = \frac{\partial}{\partial n_n} \left(\varepsilon_{\text{con}} \varpi + \frac{1}{2} \gamma T^2 \sqrt{1 - \varpi} \right). \quad (58)$$

The right hand side of (58) is readily evaluated from the assumption that the condensation energy ε_{con} and the Sommerfeld γ depend only on the total density $n = 2|\psi|^2 + n_n$, and from the explicit form of the order parameter, $\varpi = 2|\psi|^2/(2|\psi|^2 + n_n)$, giving

$$\begin{aligned} e\varphi - \lambda_{TF}^2 \nabla^2 e\varphi \\ = \chi \frac{|\psi|^2}{n} + \frac{\partial \varepsilon_{\text{con}}}{\partial n} \frac{2|\psi|^2}{n} + \frac{T^2}{2} \frac{\partial \gamma}{\partial n} \sqrt{1 - \frac{2|\psi|^2}{n}}. \end{aligned} \quad (59)$$

In the language of Jakeman and Pike, the Poisson equation (59) is called third GL equation.

The first term on the rhs of (59) is the non-local Bernoulli potential with quasiparticle screening. This can be seen if we multiply the GL equation (46) by $\bar{\psi}$ which yields

$$\chi \frac{|\psi|^2}{n} = -\frac{1}{2m^*n} \bar{\psi} (-i\hbar \nabla - e^* \mathbf{A})^2 \psi. \quad (60)$$

In the classical approximation of the kinetic energy, $(1/2m^*)\bar{\psi}(-i\hbar \nabla - e^* \mathbf{A})^2 \psi \approx \frac{1}{2}m^*v^2|\psi|^2$, one finds that the first term of (59) is the screened Bernoulli potential of van Vijfeijken and Staas, $\chi|\psi|^2/n \approx -(n_s/n)\frac{1}{2}mv^2$.

The second and third terms of (59) are non-linear generalizations of the thermodynamic correction by Rickayzen. Note that the third term remains finite at the critical point, $T \rightarrow T_c$ and $|\psi| \rightarrow 0$, yielding the normal state thermoelectric field³².

The set of GL equations is closed. It consists of the Maxwell equation (44) with the current (45), the Schrödinger equation (46) with the potential (50), and the screened Poisson equation (59). Deviations from the local charge neutrality are given by the bare Poisson equation (39).

IV. HYDRODYNAMIC PICTURE

Within the thermodynamic approach of Sec. III B, the electrostatic potential φ is a function of the wave function ψ . This contrasts with the original derivations of the Bernoulli potential expressed in terms of the condensate velocity \mathbf{v} . To make the link with the original approaches mentioned in Sec. II, in this section we reformulate the above thermodynamic theory in the hydrodynamic picture.

The hydrodynamic picture is readily obtained writing the wave function in terms of the condensate density (34) and the phase θ ,

$$\psi = \sqrt{\frac{n_s}{2}} e^{i\theta}. \quad (61)$$

A velocity defined via the current, $\mathbf{j} = en_s \mathbf{v}$, then reads

$$\mathbf{v} = \frac{1}{m^*} (\hbar \nabla \theta - e^* \mathbf{A}). \quad (62)$$

A. On Sorokin's relation

In the representation (61) the Schrödinger equation (46) reads[†]

$$\frac{1}{2}mv^2 - \frac{\hbar^2}{8m} \frac{1}{\sqrt{n_s}} \nabla^2 \sqrt{n_s} + e\varphi + w_s = 0, \quad (63)$$

where we have used $m^* = 2m$ and $\chi = 2e\varphi + 2w_s$ as it follows from (47). The thermodynamic potential w_s is given by

$$w_s = \frac{1}{2} \frac{\partial f_s}{\partial |\psi|^2}, \quad (64)$$

which is equivalent to (15). With the non-local correction neglected, $\nabla^2 \sqrt{n_s} \approx 0$, equation (63) turns into the Sorokin result (17).

Naturally, the explicit evaluation of the electrostatic potential within the Sorokin approach parallels the non-local approach presented in the previous section. Since this approach is quite transparent, we show this procedure in detail.

Relation (50) reads

$$e\varphi + w_s = -\frac{\varepsilon_{\text{con}}}{n} + \frac{\gamma T^2}{4n} \frac{1}{\sqrt{1 - \frac{n_s}{n}}}. \quad (65)$$

Substituting (65) into the local approximation of (63) one finds

$$\frac{1}{2}mv^2 = \frac{\varepsilon_{\text{con}}}{n} - \frac{\gamma T^2}{4n} \frac{1}{\sqrt{1 - \frac{n_s}{n}}}, \quad (66)$$

which yields the condensate density as a function of the local velocity. Provided that the profile of velocities in the system is known, from (66) and (59) one can directly evaluate the electrostatic potential.

[†]Equation (63) is the energy-conserving integral of motion of the Newton-like form of the Schrödinger equation. This Newton-like equation itself may be found e.g. in The Feynman Lectures on Physics³³.

B. On Rickayzen's result

Now we recover Rickayzen's result (23). To this end we have to accept identical approximations. First we neglect the Thomas-Fermi screening, so that (59) reads

$$e\varphi = \frac{n_s}{n}(e\varphi + w_s) + \frac{n_s}{n} \frac{\partial \varepsilon_{\text{con}}}{\partial n} + \frac{T^2}{2} \frac{\partial \gamma}{\partial n} \sqrt{1 - \frac{n_s}{n}}. \quad (67)$$

Second, Rickayzen assumes a local relation between the velocity and the electrostatic potential. Accordingly, we neglect the gradient correction in (63), i.e., we use the Sorokin approximation, $e\varphi + w_s = -(1/2)mv^2$, with the help of which we eliminate the Sorokin potential w_s from (67).

Third, following Rickayzen we take the limit of weak currents, $n mv^2/2 \ll \varepsilon_{\text{con}} - \gamma T^2/4$. Up to linear orders in the kinetic energy, from (66) follows $n_s = n_s^0 + n'_s$ with

$$n'_s = -n \frac{T^4}{T_c^4} \frac{n}{\varepsilon_{\text{con}}} mv^2, \quad (68)$$

so that from (67) results the electrostatic potential $\varphi = \varphi_{\text{eq}} + \varphi'$ as

$$e\varphi' = -\frac{n_s}{n} \frac{1}{2} mv^2 - \frac{\partial \varepsilon_{\text{con}}}{\partial n} \frac{n_n}{\varepsilon_{\text{con}}} mv^2 + \frac{T^2}{2} \frac{\partial \gamma}{\partial n} \frac{1}{8} \frac{n \gamma T^2}{\varepsilon_{\text{con}}^2} mv^2. \quad (69)$$

Using (30) and (22), one can rearrange expression (69) into the potential (23) derived by Rickayzen.

In summary, the result of Sorokin corresponds to the local approximation of the presented approach. The potential of Bernoulli type derived by Rickayzen includes further approximations, in particular the limit of the weak electric current. We note that for systems with vortices the non-local approach is necessary since the “classical” kinetic energy $mv^2/2$ diverges at the vortex center. This divergence is compensated by the non-local correction so that the “quantum” kinetic energy remains regular.

V. MAGNETIC PROPERTIES OF THE ABRIKOSOV VORTEX LATTICE

In this section we evaluate the wave function and the magnetic field for the Abrikosov vortex lattice in Niobium. Pure Niobium is close to the border between type-I and type-II superconductors since its GL parameter $\kappa = 0.78$ is only slightly above $1/\sqrt{2}$. However, the GL parameter can be increased up to about three by impurities. For simplicity we neglect the effect of impurities on material parameters other than the GL parameter κ .

As will be proven in the next section, deviations of the total density of electrons from its unperturbed value are very small, $|\rho| \ll \rho_{\text{latt}}$. We will neglect these deviations

and treat the material parameters in the approximation of quasi-neutrality, $\gamma(n) \approx \gamma(n_0)$ etc. In this approximation, the first and the second GL equations are independent of the third GL equation. Therefore, we shall ignore the electrostatic potential and related charge deviation within this section.

A. Dimensionless notation

Our approach parallels Ref. 34. In our calculations we shall use dimensionless quantities,

$$\begin{aligned} t &= \frac{T}{T_c}, \\ \mathbf{b} &= \frac{\lambda_{\text{Lon}} \mathbf{B}}{\lambda_0 \sqrt{B_c B_0}}, \\ \mathbf{a} &= \frac{\mathbf{A}}{\lambda_0 \sqrt{B_c B_0}}, \\ \tilde{\mathbf{r}} &= \frac{\mathbf{r}}{\lambda_{\text{Lon}}}. \end{aligned} \quad (70)$$

Close to the critical temperature, $t \rightarrow 1$, these dimensionless variables reduce to the usual form.²⁹

The thermodynamical critical field B_c , the London penetration depth λ_{Lon} , and GL parameter κ depend on the temperature as

$$\begin{aligned} B_c(t) &= B_0(1 - t^2), \\ \lambda_{\text{Lon}}(t) &= \frac{\lambda_0}{\sqrt{1 - t^4}}, \\ \kappa(t) &= \kappa_0 \sqrt{\frac{2}{1 + t^2}}, \\ B_{c2}(t) &= \sqrt{2} \kappa B_c = 2 B_0 \kappa_0 \frac{1 - t^2}{\sqrt{1 + t^2}}. \end{aligned} \quad (71)$$

The asymptotic values of these quantities in terms of the parameters of the Gorter-Casimir model read

$$\begin{aligned} B_0 &= T_c \sqrt{\frac{\mu_0 \gamma}{2}}, \\ \lambda_0 &= \sqrt{\frac{m}{e^2 n \mu_0}}, \\ \kappa_0 &= \frac{m T_c}{n e \hbar} \sqrt{\frac{\gamma}{\mu_0}}. \end{aligned} \quad (72)$$

Finally, we introduce a dimensionless amplitude of the wave function and the dimensionless velocity,

$$\begin{aligned} \omega &= \frac{2|\psi|^2}{n(1 - t^4)}, \\ \mathbf{Q} &= \mathbf{a} - \frac{1}{\kappa} \tilde{\nabla} \omega. \end{aligned} \quad (73)$$

Our dimensionless notation is identical to Ref. 34.

The Schrödinger equation (46) with the effective potential (50) in the dimensionless notation reads

$$\begin{aligned} & -\frac{1}{2\kappa^2} \tilde{\nabla}^2 \omega + \frac{(\tilde{\nabla} \omega)^2}{4\kappa^2 \omega} + \omega Q^2 \\ & = \omega - \frac{t^2}{1 - t^2} \left(\frac{1}{\sqrt{1 - (1 - t^4)\omega}} - 1 \right) \omega. \end{aligned} \quad (74)$$

The terms on the left hand side result from the kinetic energy, the terms on the right hand side represent the potential.

The Maxwell equation (44) with the current (45) reads

$$-\tilde{\nabla}^2 \mathbf{Q}_b = -\omega \mathbf{Q}_A - \omega \mathbf{Q}_b. \quad (75)$$

The full quantum velocity is a sum of two terms, $\mathbf{Q} = \mathbf{Q}_A + \mathbf{Q}_b$, where \mathbf{Q}_A is any model velocity field which covers the singular contributions at vortices,

$$\tilde{\nabla} \times \mathbf{Q}_A = \bar{\mathbf{b}} - \Phi_0 \sum_{\mathbf{R}} \delta(\tilde{\mathbf{r}} - \mathbf{R}). \quad (76)$$

In our choice of \mathbf{Q}_A appears the mean value of the magnetic field in the superconductor,

$$\bar{\mathbf{b}} = \langle \mathbf{b} \rangle = \frac{1}{\Omega} \int d\tilde{\mathbf{r}} \mathbf{b}, \quad (77)$$

therefore, for an ideally periodic vortex lattice \mathbf{Q}_A is given by the Abrikosov B_{c2} solution.³⁴ The sum over the 2D δ -functions represents the contributions of the nodes of the wave function in the vortex centers \mathbf{R} to the quantum velocity. In this choice one has $\langle \nabla \times \mathbf{Q}_b \rangle = 0$ so that $\nabla \times \mathbf{Q}_b = \mathbf{b} - \bar{\mathbf{b}}$ describes the spatial modulation of the magnetic field due to the diamagnetic currents.

B. Fourier representation

For the periodic lattice of vortices, it is advantageous to express all functions by Fourier series,

$$\omega(\tilde{\mathbf{r}}) = \sum_{\mathbf{K} \neq 0} a_{\mathbf{K}} (1 - \cos \mathbf{K} \tilde{\mathbf{r}}), \quad (78)$$

$$b(\tilde{\mathbf{r}}) = \bar{b} + \sum_{\mathbf{K} \neq 0} b_{\mathbf{K}} \cos \mathbf{K} \tilde{\mathbf{r}}. \quad (79)$$

We choose the direction of vortices along the z -axis. The function $b(\tilde{\mathbf{r}})$ is the z component of the magnetic field \mathbf{b} . Since the system is translationally invariant along z , the vectors $\tilde{\mathbf{r}} = (x, y)$ and \mathbf{K} (reciprocal lattice vectors) are two dimensional.

The special choice, $\omega \propto (1 - \cos \mathbf{K} \tilde{\mathbf{r}})$, enforces nodes of the wave function, $\omega(\mathbf{R}) = 0$, at the positions of the vortex centers, $\mathbf{R} = (ix_1 + jx_2, jy_2)$ with $i, j = 0, \pm 1, \pm 2, \dots$. For the triangular lattice, two of the nearest neighbor vortices are at $\mathbf{R} = (x_1, 0)$ and $\mathbf{R} = (x_2, y_2)$, where $x_1 = 2x_2$ and $y_2 = \sqrt{3}x_2$. The distance between vortices, x_1 , is determined by the condition that each vortex contributes to the mean magnetic field by one elementary quantum of flux, $S\bar{b} = x_1 y_2 \bar{b} = \Phi_0 = 2\pi/\kappa$. The sums

in the Fourier representation run over nonzero discrete momenta, $\mathbf{K} = (2\pi/S)(iy_2, jx_1 + ix_2)$. In this choice of the Fourier expansion the mean value of the amplitude of the wave function reads

$$\bar{\omega} = \langle \omega \rangle = \sum_{\mathbf{K} \neq 0} a_{\mathbf{K}}. \quad (80)$$

Since $\mathbf{Q}_b = \mathbf{Q} - \mathbf{Q}_A$ is periodic one may write

$$\mathbf{Q}(\tilde{\mathbf{r}}) = \mathbf{Q}_A(\tilde{\mathbf{r}}) + \sum_{\mathbf{K} \neq 0} b_{\mathbf{K}} \frac{\hat{\mathbf{z}} \times \mathbf{K}}{K^2} \sin \mathbf{K} \tilde{\mathbf{r}} \quad (81)$$

with $\hat{\mathbf{z}} \times \mathbf{K} \equiv (K_y, -K_x)$ and $\hat{\mathbf{z}}$ is the unit vector along the axis z .

C. Simple iteration scheme

Now we are ready to specify the iteration scheme for the Fourier components of the wave function and the quantum velocity.

The Fourier representation of Eq. (74) reads

$$a_{\mathbf{K}} := \frac{4\kappa^2 \langle (s - 2\omega + \omega Q^2 + g) \cos \mathbf{K} \tilde{\mathbf{r}} \rangle}{K^2 + 2\kappa^2}, \quad (82)$$

with

$$s = \frac{t^2}{1 - t^2} \left(\frac{1}{\sqrt{1 - \omega(1 - t^4)}} - 1 \right) \omega, \quad (83)$$

$$g = \frac{(\tilde{\nabla} \omega)^2}{4\kappa^2 \omega}. \quad (84)$$

The Fourier representation of Eq. (75) reads

$$b_{\mathbf{K}} := -\frac{2 \langle (\omega b + \bar{\omega}(b - \bar{b}) + p) \cos \mathbf{K} \tilde{\mathbf{r}} \rangle}{K^2 + \bar{\omega}}, \quad (85)$$

with

$$p = (\nabla \omega \times \mathbf{Q}) \hat{\mathbf{z}} = Q_x \frac{\partial \omega}{\partial y} - Q_y \frac{\partial \omega}{\partial x}. \quad (86)$$

Within a simple iteration scheme for given values of t , \bar{b} , and κ , one starts from the Abrikosov B_{c2} solution or some other values of $a_{\mathbf{K}}$ and $b_{\mathbf{K}}$. In the step (a) one evaluates $a_{\mathbf{K}}$ from (82) and upgrades $\omega(x, y)$ according to (78). In the step (b) one evaluates $b_{\mathbf{K}}$ from (85) and upgrades $b(x, y)$ and $Q(x, y)$ from (79) and (81). The iteration scheme (a), (b), (a), (b), ... then leads to the periodic solution of Eqs. (74) and (75).

D. Accelerated iteration scheme

As shown in Ref. 34, the convergence is accelerated if the amplitude of the wave function is optimized after

each use of equation (82). Here we show how to make this optimization within the Bardeen set of equations.

Assume a change of the wave function $\omega(x, y)$ which maintains its shape but modifies its amplitude,

$$\omega(x, y) := (1 + c)\omega(x, y), \quad (87)$$

i.e., the old value ω (the right hand side) obtained from (82) is replaced by a new value.

The constant c has to be found at each iteration step from the minimum of the free energy. Since we neglect the Coulomb interaction in this part of the treatment, we can also eliminate the internal energy U . The free energy normalized as

$$\tilde{f} = \frac{f_s - U + f_{\text{kin}} + f_M}{\frac{1}{4}\gamma T_c^2(1 - t^2)(1 - t^4)}, \quad (88)$$

in the dimensionless representation reads

$$\tilde{f} = -\frac{\omega}{1 - t^2} - \frac{2t^2 \sqrt{1 - \omega(1 - t^4)}}{(1 - t^2)(1 - t^4)} + (\tilde{\nabla} \times \mathbf{Q} - b_a)^2 + \omega Q^2 + \frac{(\tilde{\nabla} \omega)^2}{4\kappa^2 \omega}. \quad (89)$$

When we substitute (87) into (89), the variation with respect to c , $\partial \langle \tilde{f} \rangle / \partial c = 0$, yields the condition for c as

$$\begin{aligned} & \left\langle -\frac{\omega}{1 - t^2} + \omega Q^2 + \frac{(\tilde{\nabla} \omega)^2}{4\kappa^2 \omega} \right\rangle \\ &= - \left\langle \frac{t^2}{1 - t^2} \frac{\omega}{\sqrt{1 - (1 + c)\omega(1 - t^4)}} \right\rangle. \end{aligned} \quad (90)$$

Condition (90) is not convenient for the numerical treatment. When the starting value of the wave function is reasonable, or after a few iteration steps (a), (b), (a), (b), the correction c will be small, $c \ll 1$, so that the linear approximation of (90) is sufficient,

$$c = -\frac{2 \langle s - \omega + \omega Q^2 + g \rangle}{t^2(1 + t^2) \langle \omega^2 (1 - \omega(1 - t^4))^{-\frac{3}{2}} \rangle}. \quad (91)$$

As a third iteration step (c) we thus may use Eq. (87) with c given by (91). The iteration procedure we use starts from a preliminary adjustment of the wave function by a few steps, (a), (c), (a), (c), ..., putting $b_{\mathbf{K}} \equiv 0$. After that the full iteration scheme (a), (c), (b), (a), (c), (b), ... is applied yielding all Fourier coefficients $a_{\mathbf{K}}$, $b_{\mathbf{K}}$.

E. Magnetic properties

In Figs. 1-4 we present some numerical results to illustrate the properties of the Bardeen equations. As one can see from the dimensionless equations (74) and (75), the behavior of the system is determined by a single material parameter, the GL parameter κ . We assume Niobium

doped with non-magnetic impurities of a density giving the GL parameter $\kappa_0 = 1.5$.

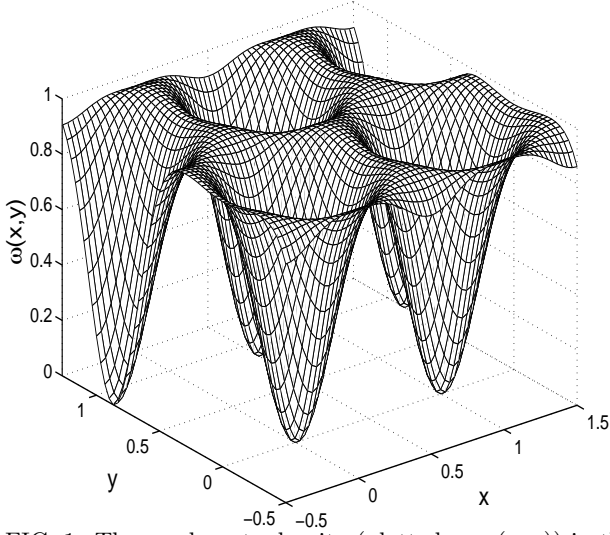


FIG. 1. The condensate density (plotted as $\omega(x, y)$) in the triangular lattice for temperature $t = 0.5$, magnetic induction $\bar{B}/B_{c2} = 0.5$, and GL parameter $\kappa_0 = 1.5$. In the vortex centers the condensate density $n_s(x, y)/n = (1 - t^4)\omega(x, y)$ goes to zero. Between the vortices $\omega(x, y)$ approaches its equilibrium value 1 (which would be constant in the absence of a magnetic field) yielding $n_s^{\text{eq}}/n = 1 - t^4 = 0.94$.

Figure 1 shows a fishnet plot of the condensate density $n_s(x, y)/n = (1 - t^4)\omega(x, y)$ for temperature $t = T/T_c = 0.5$ and the mean magnetic field $\bar{B} = 0.5 B_{c2}$. The dips in n_s correspond to the nodes of the wave function ψ located at the vortex centers. The condensate density reaches its maximum between the vortices.

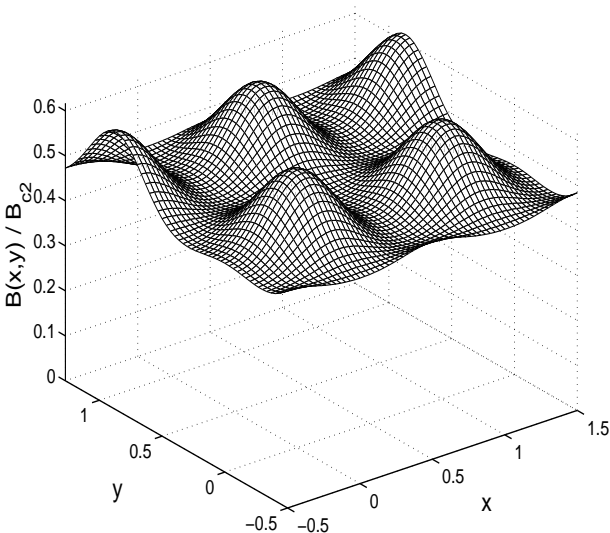


FIG. 2. The magnetic field in units of the upper critical field B_{c2} for $t = 0.5$, $\bar{B}/B_{c2} = 0.5$, and $\kappa_0 = 1.5$ as in Fig. 1. $B(x, y)$ reaches its maximum B_{max} at the vortex centers.

Note that the condensate density is smaller than its non-magnetic value, $n_s^0 = n(1 - T^4/T_c^4)$, also on the borders of the elementary cells where the current is zero. This shows that non-local effects given by gradient corrections, e.g. the second term of (63), are important not only at the vortex core but also between the vortices.

A complementary picture offers the plot of the magnetic field B presented in Fig. 2. The magnetic field reaches its maximum value, B_{max} , at the vortex centers. This maximum field is very close to but slightly higher than the applied field B_a because the superconductor tries to expel the magnetic field and compresses it into vortices. The magnetic pressure on the condensate is one of the forces balanced by the electric field.

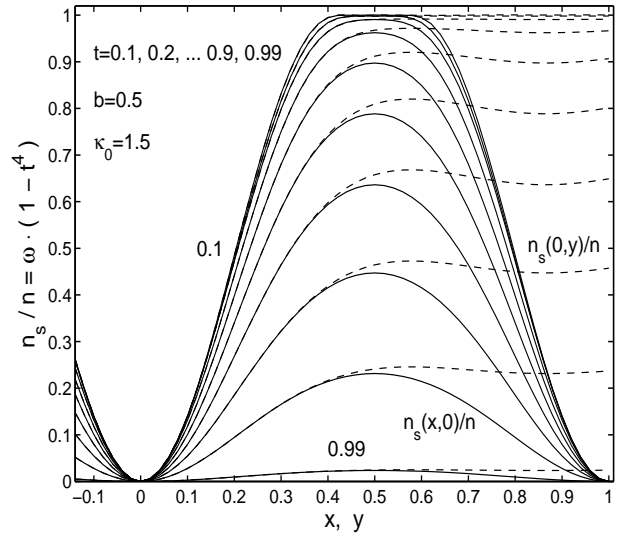


FIG. 3. Profiles of the condensate density $n(x, y)$ at various temperatures for $\bar{B}/B_{c2} = 0.5$ and $\kappa_0 = 1.5$. The solid lines show cuts along the x -axis, and the dashed lines along the y -axis.

The temperature dependence of the condensate density $n_s(x, y)/n = (1 - t^4)\omega(x, y)$ is shown in Fig. 3. As one expects, the density of the condensate decreases as the temperature approaches the critical value, $t \rightarrow 1$. The dominant part of this decrease can be attributed to the reduced fraction of the condensate expressed by the factor $(1 - t^4)$. We have numerically checked that near the critical temperature the condensate density results identical to the solution of the standard GL theory.

In Fig. 4, the density of the condensate is normalized to its value in absence of the magnetic field, $n_s(x, y)/n_s^0 = \omega(x, y)$. The suppression of $\omega(x, y)$ in the region between the vortices is completely due to the magnetic field. One can see that at lower temperatures the condensate is less suppressed than it would result from the GL theory, where the latter one is equal to the curve at $t = 0.99$. This follows from the fact that the condensation energy \mathcal{F}_s increases with the condensate density slower than the quadratic function of the GL theory.

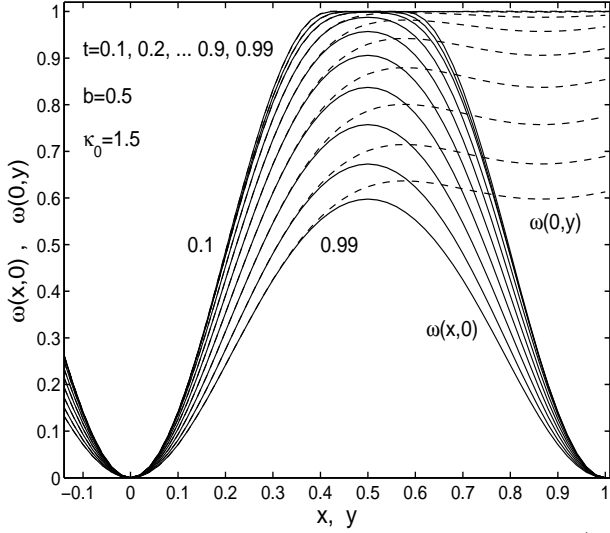


FIG. 4. Profiles of the reduced condensate density $\omega(x, y)$ at various temperatures $t = T/T_c$ for $\bar{B}/B_{c2} = 0.5$ and $\kappa_0 = 1.5$ as in Fig. 3.

F. Virial theorem

In the above treatment, the magnetic field was specified by the mean value \bar{B} of the magnetic induction in the sample. Macroscopic magnetic properties of the system, however, are given by the magnetization M . Let us link these two quantities.

For simplicity we assume that the sample is an infinite cylinder in the direction of the applied field. In this longitudinal geometry one has $\bar{B} = B_a + M$. Since the non-local terms of the free energy are terminated at the second-order derivatives (the term called kinetic energy), we can conveniently use the virial theorem derived by Doria, Gubernatis and Rainer³⁵ and generalized by Klein and Pöttinger³⁶, to evaluate the applied magnetic field B_a .

The idea of the virial theorem is as follows. Let us introduce a parameter ι which scales coordinates x and y . With this scaling one can generate a new wave function $\omega'(\mathbf{r}) = \omega(\iota\mathbf{r})$. Since the mean magnetic field is given by the density of vortices, it scales as $\bar{B}'(\mathbf{r}) = \iota^{-2}\bar{B}(\iota\mathbf{r})$. We rescale all magnetic fields with ι^{-2} except for the applied field B_a which is an external parameter.

From $\mathbf{B} = \nabla \times \mathbf{A}$ one can see that the vector potential scales as $\mathbf{A}'(\mathbf{r}) = \iota^{-1}\mathbf{A}(\iota\mathbf{r})$, i.e., in the same way as a gradient. Accordingly, the density of kinetic energy scales with ι^{-2} . The mean value of free energy corresponding to the new wave function reads

$$\begin{aligned} \langle f' \rangle = & \left\langle -\frac{\omega}{1-t^2} - \frac{t^2\sqrt{1-\omega(1-t^4)}}{(1-t^2)(1-t^4)} \right\rangle \\ & + \iota^{-2} \left\langle \omega Q^2 + \frac{(\tilde{\nabla}\omega)^2}{4\kappa\omega} \right\rangle + \left\langle (\iota^{-2}\tilde{\nabla} \times \mathbf{Q} - b_a)^2 \right\rangle. \end{aligned} \quad (92)$$

The condensation energy (the first term) is independent of the scaling. The kinetic energy (the second term) scales with ι^{-2} . The magnetic energy (the third term) has three contributions: $\langle b^2 \rangle = \langle (\nabla \times \mathbf{Q})^2 \rangle$ which scales with ι^{-4} ; $-2\bar{b}b_a = -2\langle (\nabla \times \mathbf{Q})b_a \rangle$ which scales with ι^{-2} ; and b_a^2 which is independent of the scaling.

Since the scaling deforms the wave function and the internal magnetic field from their equilibrium values, the free energy $\langle f' \rangle$ is greater than the free energy $\langle \tilde{f} \rangle$. For $\iota = 1$ the free energy $\langle f' \rangle$ reaches its minimum being equal to $\langle \tilde{f} \rangle$. This minimum is given by a variation with respect to ι ,

$$\left. \frac{\partial}{\partial \iota} \langle f' \rangle \right|_{\iota=1} = 0. \quad (93)$$

Condition (93) in the explicit form,

$$2\bar{b}b_a = \left\langle \omega Q^2 + \frac{(\tilde{\nabla}\omega)^2}{4\kappa\omega} \right\rangle + 2\langle (\nabla \times \mathbf{Q})^2 \rangle, \quad (94)$$

is called the virial theorem. Since \bar{b} , ω and \mathbf{Q} are known, the virial theorem (94) provides us with the value of the applied magnetic field b_a without having to take the derivative of the computed free energy.

A convenient form of the virial theorem valid only for the Bardeen equations makes use of the Schrödinger equation (74) from which follows

$$\left\langle \omega Q^2 + \frac{(\nabla\omega)^2}{4\kappa\omega} \right\rangle = \langle \omega - s \rangle \quad (95)$$

with s from (83). The applied magnetic field then reads

$$b_a = \frac{\langle 2b^2 + \omega - s \rangle}{2\bar{b}}. \quad (96)$$

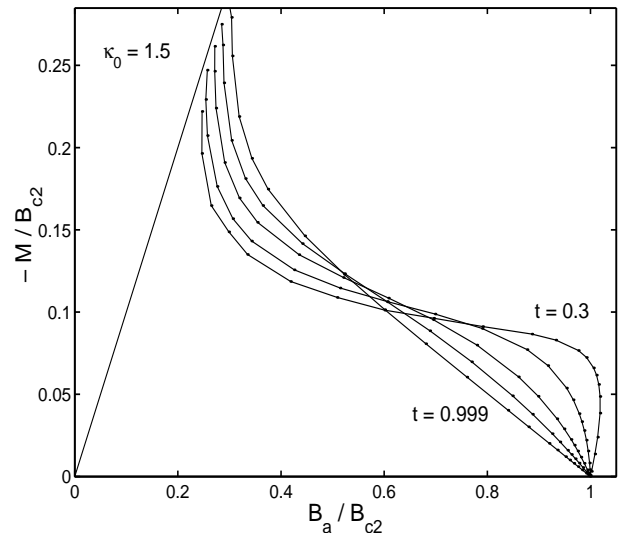


FIG. 5. The magnetization $-M = B_a - \bar{B}$ as a function of the applied magnetic field B_a in units of the upper critical field B_{c2} at temperatures $t = 0.999, 0.85, 0.7, 0.5, 0.3$ for $\kappa_0 = 1.5$.

The magnetization $-M = B_a - \bar{B}$ as a function of the applied magnetic field B_a is shown in Fig. 5 for different temperatures. At temperatures close to T_c the magnetization follows the line well known from the GL theory. Below the lower critical field B_{c1} the system is in the Meissner state and $-M = B_a$. Above B_{c1} the magnetization decreases and linearly vanishes at B_{c2} where the system undergoes a transition into the normal state.

At very low temperatures, the magnetization is deformed into an S-shape. The slope of the decrease, $\partial M / \partial B_a$, close to B_{c2} increases with decreasing temperature and at a certain temperature T_a becomes infinite. Below T_a , the magnetic behavior of the system achieves an anomalous feature. As the magnetic field is lowered from some high value, the system undergoes a first order transition from zero to a finite magnetization at a field which is above B_{c2} . Since the free energy of the system with finite magnetization is lower than the free energy of the normal state, the system jumps to a finite magnetization as soon as the applied magnetic field allows for such solution.

Such anomalous magnetic transition has been observed by Ehrat and Rinderer^{37,38} for Lead doped with Niobium. In spite of this experimental result we believe that the first order transition seen in Fig. 5 is an artifact of the Bardeen approximation. Indeed, detailed theoretical discussions^{39–41} of this anomalous behavior point to the important role of scattering on impurities. This mechanism is absent in the Bardeen approximation.

The temperature T_a can be determined from the Bardeen equations. Close to the critical field B_{c2} the density of condensate is small and one can expand the effective potential (50) into the GL form (51) with coefficients

$$\alpha = \frac{\gamma}{2n}(T^2 - T_c^2), \quad \beta = \frac{\gamma T^2}{2n^2}. \quad (97)$$

For these asymptotic values one can introduce an asymptotic GL parameter,²⁹

$$\kappa_{as} = \sqrt{\frac{m^2 \beta}{2\mu_0 \hbar^2 e^2}}. \quad (98)$$

As one can see from (97), this asymptotic GL parameter decreases with the temperature,

$$\kappa_{as} = \kappa_0 t. \quad (99)$$

The transition temperature T_a appears when the effective GL parameter equals to $1/\sqrt{2}$, i.e.,

$$T_a = \frac{T_c}{\sqrt{2}\kappa_0}. \quad (100)$$

For $\kappa_0 = 1.5$ one finds $T_a = 0.47 T_c$. We expect that one should be cautious about results of the Bardeen equations below T_a .

Let us return to features related to the electrostatic forces. As mentioned above, in the vortex core the magnetic field $B(x, y)$ is compressed and thus exceeds the value of the applied field B_a . In Fig. 6 we compare the applied field with the field B_{\max} in the center of the vortex. For all temperatures the compression is stronger at lower magnetic fields.

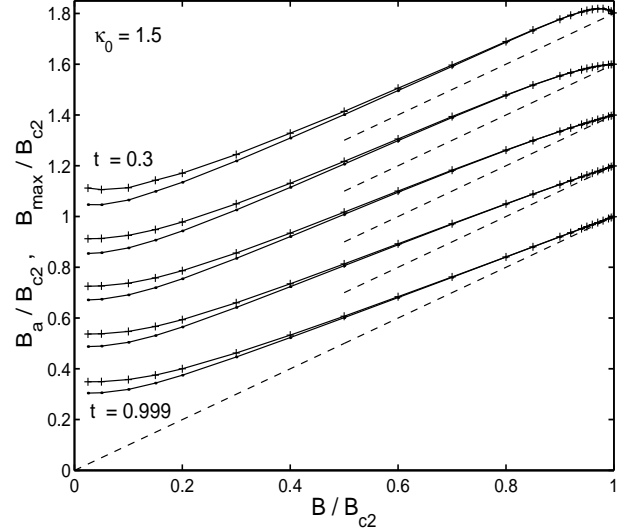


FIG. 6. The applied field B_a (solid lines with dots) and the field B_{\max} in the vortex center (solid lines with crosses) plotted versus the induction \bar{B} for $\kappa_0 = 1.5$ at temperatures $t = 0.999, 0.85, 0.7, 0.5, 0.3$ as in Fig. 5. For clarity, each line pair of the next temperature is shifted up by 0.2. The dashed lines indicate the large- κ -limit $B_a = \bar{B}$.

VI. ELECTROSTATIC POTENTIAL AND CHARGE IN THE ABRIKOSOV LATTICE

The electrostatic potential, φ , together with the Sorokin thermodynamic potential, w_s , control the motion of Cooper pairs. Indeed, the total effective potential acting on the Cooper pairs is $\chi = e^* \varphi + 2w_s$. The separation of the effective potential χ into its electrostatic and thermodynamic components sheds a light on the role of the electrostatic potential in the Schrödinger equation (18) or (46).

A. Electrostatic potential

The electrostatic potential in the vortex lattice is given by the screened Poisson equation (59). For simplicity we neglect the screening, putting $\lambda_{TF}^2 \nabla^2 e \varphi = 0$. This approximation is justified below.

To be compatible with the above notation, we define a dimensionless electrostatic potential,

$$\phi = \frac{en}{\frac{1}{4}\gamma T_c^2(1-t^2)(1-t^4)} \varphi. \quad (101)$$

With the screening neglected one finds from (59)

$$\phi = s - \omega + C_1\omega + C_2\sqrt{1 - (1 - t^4)\omega}, \quad (102)$$

with temperature dependent factors

$$C_1 = \frac{1}{1 - t^2} \frac{\partial \ln \varepsilon_{\text{con}}}{\partial \ln n}, \quad (103)$$

and

$$C_2 = \frac{1}{1 - t^2} \frac{\partial \ln \gamma}{\partial \ln n}. \quad (104)$$

The term $s - \omega$ in (102) corresponds to $\chi|\psi|^2/n$ in (59). The $C_{1,2}$ terms correspond to the second and third terms of (59), respectively.

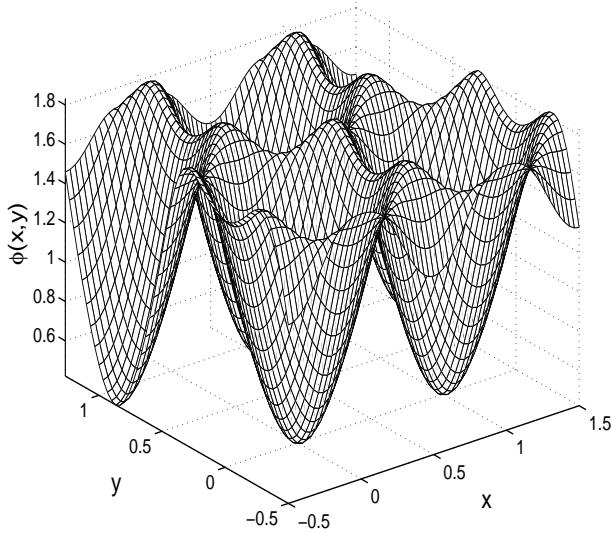


FIG. 7. The electrostatic potential $\phi(x, y)$, Eq. (101). The temperature $t = 0.5$, the magnetic field $\bar{B}/B_{c2} = 0.5$ and the GL parameter $\kappa_0 = 1.5$ are identical to the values used in Figs. 1 and 2. The thermodynamic coefficients C_1 and C_2 are specified in Tab. 1.

Figure 7 shows a fishnet plot of the electrostatic potential. The potential reaches its minimum at the vortex centers, i.e., it attracts electrons to vortices.

The total electrostatic potential ϕ is composed of three components: the Bernoulli potential $\phi_B = s - \omega$, the contribution due to the condensation energy $\phi_1 = C_1\omega$ and the reduced normal state thermoelectric potential $\phi_2 = C_2\sqrt{1 - (1 - t^4)\omega}$. Individual components are compared in Fig. 8.

The Bernoulli potential ϕ_B shown in Fig. 8 is negative. Due to the quasiparticle screening, the Bernoulli potential reaches zero at the center of the vortex. With respect to the center of the vortex, the forces corresponding to the Bernoulli potential are repulsive inside the core while they are attractive outside.

The potential ϕ_1 caused by the density dependence of the condensation energy is positive. Being proportional

to the density of condensate, it has a minimum at the vortex center where it reaches zero. For Niobium this contribution is dominant since the coefficient $C_1 = 1.9$ is rather large compared to the coefficients of other contributions.

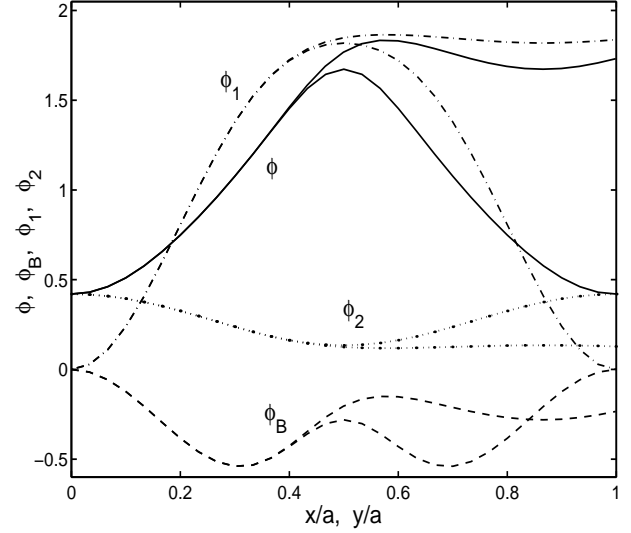


FIG. 8. The components of the electrostatic potential in the vortex lattice of spacing a according to Eq. (102). The individual potentials are: the total potential ϕ (solid lines), the Bernoulli potential $\phi_B = s - \omega$ (dashed lines), the condensation potential $\phi_1 = C_1\omega$ (dashed-dotted lines), and the normal thermodynamic potential $\phi_2 = C_2\sqrt{1 - (1 - t^4)\omega}$ (dotted lines). The splitting of lines at larger distances characterizes the x -direction (lower curves) or y -direction (upper curves). Parameters as in Fig. 7.

The normal state thermodynamic potential ϕ_2 is also positive giving the only non-zero contribution at the vortex center. One can see that ϕ_2 reduces the total potential since it has the maximum at the vortex core and falls outside. Its coefficient $C_2 = 0.42$ is about four times smaller than C_1 , therefore this term cannot cancel the potential ϕ_1 .

We want to stress that even at temperature $t = 0.5$ when 96% of electrons are in the condensate, the thermodynamic correction to the electrostatic potential cannot be neglected. This result contradicts the temperature dependence of the thermodynamic correction derived by Rickayzen²², see Eq. (23). Within the hydrodynamic picture one can show that the limit of weak currents adopted by Rickayzen is responsible for this disagreement. In this limit, the effect of the diamagnetic current on the condensate density n_s vanishes as $T \rightarrow 0$, see Eq. (68). The temperature dependence of the thermodynamic correction merely reflects the temperature dependence of n'_s . The limit of weak current does not apply to the vortex core. In the center of the vortex core, the condensate density has to go to zero keeping the magnitude of the thermodynamic correction appreciable at any temperature.

B. Effective potential

To enlighten the role of the electrostatic potential in the balance of forces in superconductors, we compare the effective potential χ , the electrostatic potential acting on the Cooper pair $e^*\varphi$, and the thermodynamic potential of Sorokin $2w_s$ in Fig. 9. All these contributions are in dimensionless units corresponding to (101).

One can see that the electrostatic potential is not a small correction to the effective potential of a thermodynamic origin. The amplitude of the electrostatic potential is about an order of magnitude larger than the amplitude of the effective potential χ . Accordingly, the effective potential $\chi = e^*\varphi + 2w_s$ results from a strong compensation of the thermodynamic potential $2w_s$ and the electrostatic potential $e^*\varphi$.

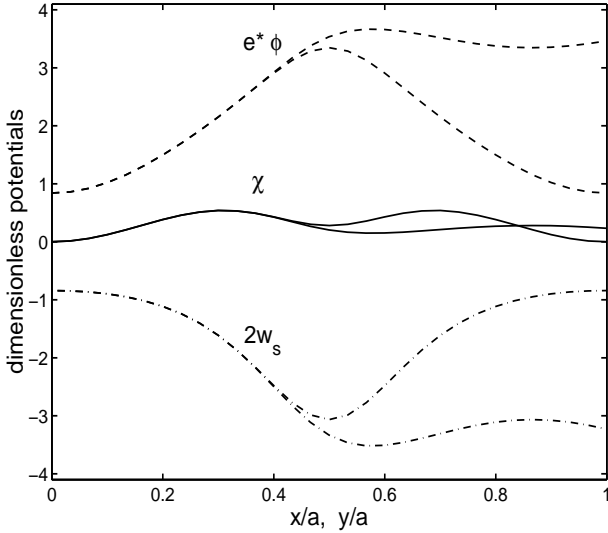


FIG. 9. The effective potential $\chi = e^*\varphi + 2w_s$ (full lines), the electrostatic potential acting on the Cooper pair $e^*\varphi$ (dashed lines) and the thermodynamic potential $2w_s$ (dash-dotted lines) for $\kappa_0 = 1.5$. Parameters and presentation as in Fig. 8.

C. Charge

The distribution of the charge in the vortex lattice is given by the Poisson equation, $\rho = -\epsilon \nabla^2 \phi$. We introduce a dimensionless charge,

$$\tilde{\rho} = \frac{\rho}{en}, \quad (105)$$

which measures the relative deviation of the charge density from the crystal value. In dimensionless representation the Poisson equation reads

$$\tilde{\rho} = -C_3 \frac{\lambda_{TF}^2}{\lambda_{Lon}^2} \tilde{\nabla}^2 \phi, \quad (106)$$

with

$$C_3 = \frac{2\mathcal{D}\varepsilon_{con}}{n^2}(1-t^2)(1-t^4). \quad (107)$$

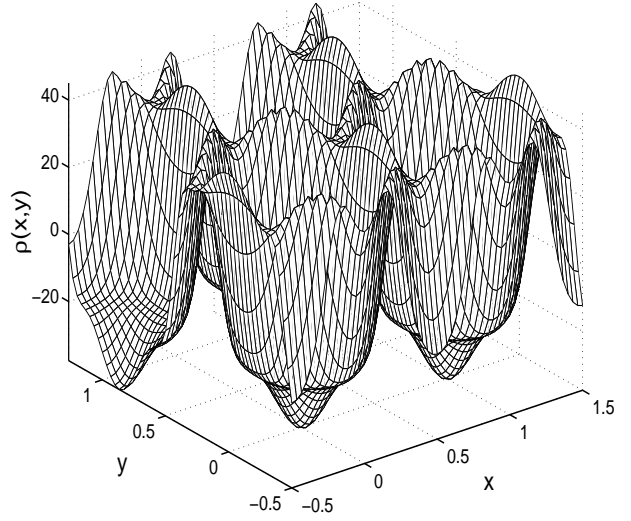


FIG. 10. The function $-\nabla^2 \phi$ proportional to the charge density $\rho(x, y)$. The amplitude of the dimensionless charge density is $\tilde{\rho} = 9.5 \cdot 10^{-11} \cdot (1-t^2)(1-t^4)^2 \tilde{\nabla}^2 \phi$. Same parameters as in Figs. 7, 8, 9.

Figure 10 shows a fishnet plot of the charge distribution. In the vortex core the charge is depleted, the missing charge is distributed between vortices.

A striking feature is the very rapid change of the charge sign at the distance about 0.4 from the vortex center. While the charge in the core is rather flat, its spatial variation between vortices is quite strong. This picture of the charge distribution is just opposite to the one assumed by Kumagai, Nozaki and Matsuda¹⁰ who expected a flat charge distribution between vortices. Comparing these two pictures, however, one has to keep in mind that Kumagai *et al* discuss YBCO with $\kappa \sim 100$ while Fig. 10 presents the case of $\kappa_0 = 1.5$ in Niobium.

The particular shape of the charge seen in Fig. 10 results from the interplay between the Bernoulli potential ϕ_B and the potential ϕ_1 due to the condensation energy. In Fig. 11, we show the charge density decomposed into contributions corresponding to individual potentials, $\rho_i \propto \nabla^2 \phi_i$.

The charge distribution ρ_B corresponding to the Bernoulli potential ϕ_B has its maximum at the center of the vortex. In Ref. 21, where only the non-local (quantum) Bernoulli potential has been assumed, there is a minimum of the charge density in the center of vortex. The local maximum seen in Fig. 11 follows from the quasiparticle screening not assumed in Ref. 21.

The amplitudes of the contributions ρ_1 and ρ_2 depend on the constants C_1 and C_2 , which strongly depend on the material in question. For Niobium one has $C_1 = 1.9$ and $C = 0.42$; therefore ρ_1 dominates. In Appendix A one can see that both constants C_1 and C_2 are propor-

tional to the slope of the density of states at the Fermi level. In general one can say that the amplitude of ρ_2 is smaller than the amplitude of ρ_1 and the two contributions have opposite signs of the periodic parts. We note that due to the large value of C_1 and small C_2 , the total charge has a minimum in the center of the vortex.

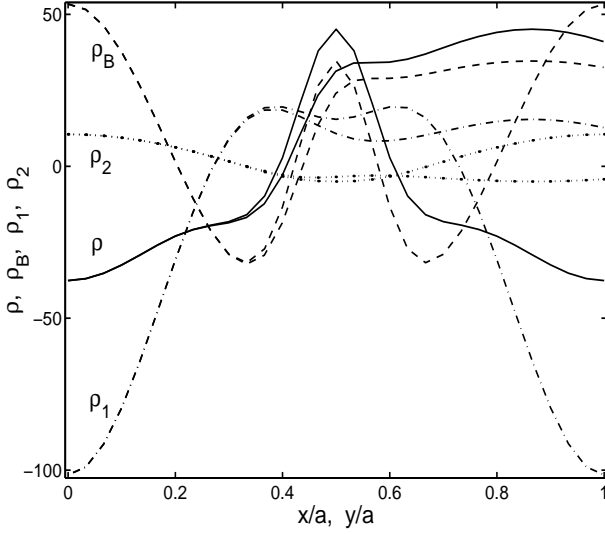


FIG. 11. The components of the charge density in the notation of Fig. (8) for same parameters. The individual charge densities are: the total ρ (solid lines), the Bernoulli ρ_B (dashed lines), the condensation part ρ_1 (dash dotted lines), and the normal thermodynamic part ρ_2 (dotted lines).

D. Screening and the quasi-neutral approximation

For Niobium, the Thomas-Fermi screening length is very small,

$$\frac{\lambda_{TF}^2}{\lambda_{Lon}^2} = 2.5 \cdot 10^{-6} (1 - t^4). \quad (108)$$

One can thus neglect the screening, $\lambda_{TF}^2 \lambda_{Lon}^{-2} \nabla^2 \phi \ll \phi$. Indeed, the Laplace operator in the Fourier representation is $\nabla^2 \rightarrow K^2 = (4\pi/\sqrt{3})\kappa\bar{b}(i^2 + j^2)$. Since κ is of the order of unity, $\bar{b} < 1$ and the number of needed Fourier components is also limited, $i, j < 100$, the screening is negligible for all Fourier components considered.

For Niobium, the factor

$$\frac{2\mathcal{D}\varepsilon_{con}}{n^2} = 3.8 \cdot 10^{-5} \quad (109)$$

which determines C_3 in (106), is also very small. Similarly small value can be expected for any conventional superconductor. It leads to relative charges of the order of 10^{-10} . The quasi-neutral approximation, $\gamma(n) \approx \gamma(n_0)$ etc., is thus well justified when one solves for the wave function and the vector potential.

VII. CONCLUSIONS

In this paper we have discussed the electrostatic potential in the Abrikosov lattice of vortices. To this end we have derived a set of three Ginzburg-Landau equations which include the Maxwell equation for the vector potential, the Schrödinger equation for the wave function, and the Poisson equation for the electrostatic potential. These equations determine the minimum of the free energy made of four components: the condensation energy of Gorter and Casimir; the quantum kinetic energy of Ginzburg and Landau; the magnetic free energy of Helmholtz; and the Coulomb energy.

The marriage of the Gorter-Casimir two-fluid model with the Ginzburg-Landau theory has been suggested earlier by Bardeen who has also discussed properties of this theory at different temperature limits. We have employed his approach as it offers a very simple extension of the GL theory towards low temperatures. As our results document, this extended theory can be treated with standard numerical tools of the GL theory.

With the electrostatic interaction included, the effective potential acting on the superconducting condensate is naturally a sum of the electrostatic potential and the thermodynamic potential. One can say that the electrostatic potential (over-)screens the thermodynamic potential leaving a relatively small effective potential.

In spite of the very important role of the electrostatic potential among forces acting on the condensate, the electrostatic potential can be eliminated from the Ginzburg-Landau theory so that one has to solve a set of two, not three, equations. This simplification is possible by two reasons. First, the charge modulation which corresponds to this potential, is so small on the scale of the charge density in metals that one can neglect its effect on local values of material parameters.

The second reason is more fundamental. As noticed by van Vijfeijken and Staas, there is a force between the condensate and the normal electrons. This force keeps the normal electrons at rest, i.e., it balances the electric field having an equal amplitude and the opposite orientation. The force of van Vijfeijken and Staas is an exclusive function of the condensate density. Accordingly, one can express the electric force or the electrostatic potential as a function of the condensate density. In this way the electrostatic potential can be unified with the thermodynamic potential into an effective potential of GL-type.

In the numerical treatment we have used the parameters of Niobium. Our choice of this conventional material was determined by known empirical rules needed to predict amplitudes of the individual contributions to the electrostatic potential. We expect that other d-band superconductors behave similarly.

Finally, we would like to stress that the presented theory is simplified in many directions. First, it is restricted to isotropic materials. We have omitted all features of the band structure except for the density of states and

its slope on the Fermi level. Second, the two-fluid model of Gorter and Casimir describes only gross features of the thermodynamics of superconductors. Third, the gradient approximation of the Ginzburg-Landau theory is justified only close to the critical temperature, at low temperatures one has to take the kinetic energy of Ginzburg and Landau as an ad hoc approximation. In the future, we plan to address layered structures and use a more general form of the Gorter-Casimir model.

APPENDIX A: ESTIMATE OF MATERIAL PARAMETERS FOR NIOBIUM

In this appendix we estimate material parameters, $\partial\gamma/\partial n$ and $\partial\varepsilon_{\text{con}}/\partial n$, which determine the electrostatic potential in the superconductor, see (59). To be specific we assume Niobium.

1. Coefficient $\partial\gamma/\partial n$

The linear coefficient of the specific heat γ is linked to the density of states \mathcal{D} per spin and unitary volume,

$$\gamma = \frac{2}{3}\pi^2 k_B^2 \mathcal{D}. \quad (\text{A1})$$

It is advantageous to express the density derivative of γ in terms of the energy derivative of the density of states. Using $\partial E_F/\partial n = 1/2\mathcal{D}$ we find

$$\frac{\partial\gamma}{\partial n} = \frac{1}{3}\pi^2 k_B^2 \frac{\partial \ln \mathcal{D}}{\partial E_F}. \quad (\text{A2})$$

The density of states \mathcal{D} includes the mass renormalization due to the electron-phonon interaction,⁴²

$$\mathcal{D} = \mathcal{D}_0(1 + \lambda), \quad (\text{A3})$$

where \mathcal{D}_0 is a bare density of states and λ is the coupling parameter. The value and the energy derivative of \mathcal{D}_0 is provided by *ab initio* studies of Niobium.⁴³

The value of the coupling parameter λ is found comparing \mathcal{D} from the experimental γ with the theoretical \mathcal{D}_0 . The energy derivative of λ , however, is not provided in the literature. To estimate the derivative of λ we write it as a product,

$$\lambda = \mathcal{D}_0 V, \quad (\text{A4})$$

where V is the BCS interaction.

According to trends found from the effects of impurities on the critical temperature and the specific heat, the major changes of λ follow from the density of states while the BCS interaction V remains nearly constant.⁴⁴ As a first approximation we thus assume

$$\frac{\partial V}{\partial n} = 0 \quad \text{or} \quad \frac{\partial V}{\partial E_F} = 0. \quad (\text{A5})$$

Now we can complete the estimate of $\partial\gamma/\partial n$. From (A3-A5) follows

$$\frac{\partial\mathcal{D}}{\partial E_F} = (1 + 2\lambda) \frac{\partial\mathcal{D}_0}{\partial E_F}, \quad (\text{A6})$$

therefore relation (A2) can be expressed as

$$\frac{\partial\gamma}{\partial n} = \frac{1}{3}\pi^2 k_B^2 \frac{1 + 2\lambda}{1 + \lambda} \frac{\partial \ln \mathcal{D}_0}{\partial E_F}. \quad (\text{A7})$$

2. Coefficient $\partial\varepsilon_{\text{con}}/\partial n$

The derivative of the condensation energy (30) includes the derivative of the critical temperature. For Niobium and similar materials the critical temperature is given by the McMillan formula,⁴²

$$T_c = \frac{\theta_D}{1.45} \exp \left[-\frac{1.04(1 + \lambda)}{\lambda - \mu^*(1 + 0.62\lambda)} \right], \quad (\text{A8})$$

where θ_D is the Debye temperature and μ^* is the Coulomb pseudopotential. From (30) and (A8) we express the condensation energy as

$$\varepsilon_{\text{con}} = \frac{\pi^2}{12.6} k_B^2 (1 + \lambda) \mathcal{D}_0 \theta_D^2 \exp \left[-2 \frac{1.04(1 + \lambda)}{\lambda - \mu^*(1 + 0.62\lambda)} \right]. \quad (\text{A9})$$

Experience from dilute alloys shows that the product $\mathcal{D}_0 \theta_D^2$ is nearly constant.⁴⁴ We thus use as the second approximation,

$$\frac{\partial}{\partial n} \mathcal{D}_0 \theta_D^2 = 0. \quad (\text{A10})$$

In this approximation the derivative of the condensation energy is given by the derivative of the factor $1 + \lambda$ and by the derivative of the argument of the exponential,

$$\frac{\partial\varepsilon_{\text{con}}}{\partial n} = \varepsilon_{\text{con}} \frac{\partial}{\partial n} \left(-\frac{2.08(1 + \lambda)}{\lambda - \mu^*(1 + 0.62\lambda)} + \ln(1 + \lambda) \right). \quad (\text{A11})$$

Again, the experience with dilute alloys shows that the Coulomb pseudopotential is nearly constant,⁴⁴ therefore we take as the third approximation,

$$\frac{\partial\mu^*}{\partial n} = 0. \quad (\text{A12})$$

With approximation (A12) the density derivative of the condensation energy becomes proportional to the derivative of the coupling parameter,

$$\frac{\partial\varepsilon_{\text{con}}}{\partial n} = \varepsilon_{\text{con}} \frac{\partial\lambda}{\partial n} \left(\frac{2.08(1 + 0.38\mu^*)}{(\lambda - \mu^*(1 + 0.62\lambda))^2} + \frac{1}{1 + \lambda} \right). \quad (\text{A13})$$

The density derivative of the coupling constant follows from (A4) and approximation (A5) as

$$\frac{\partial \lambda}{\partial n} = \frac{V}{2(1+\lambda)} \frac{\partial \ln \mathcal{D}_0}{\partial E_F}. \quad (\text{A14})$$

The derivative of the condensation energy is thus proportional to the BCS interaction,

$$\frac{\partial \varepsilon_{\text{con}}}{\partial n} = \frac{\varepsilon_{\text{con}} V}{(1+\lambda)^2} \frac{\partial \ln \mathcal{D}_0}{\partial E_F} \left(\frac{1.04(1+0.38\mu^*)(1+\lambda)}{(\lambda - \mu^*(1+0.62\lambda))^2} + \frac{1}{2} \right). \quad (\text{A15})$$

The material parameters for Niobium which we have used are listed in Table 1. For convenience, we have included values which can be evaluated from the above formulas, e.g., the critical temperature is given by (A8). The logarithmic derivative of the density of states with respect to the energy is extracted from the figure in Ref. 43. The hole density n has been evaluated from the London penetration depth⁴⁵

$$\lambda_{\text{Lon}}^2 = \frac{m}{n_s e^2 \mu_0}. \quad (\text{A16})$$

At zero temperature all holes are in the condensate, $n = n_s$. The listed density of holes follows from $\lambda_{\text{Lon}} = \lambda_0 = 3.9 \cdot 10^{-8} \text{ m}$ and the mass $m_0 = 1.2 m_e$. This effective mass is an estimate of values 1.12, 1.6, 1.28 and 1.22 for different orbits of the pure Niobium.⁴⁶

We assume that the properties of the material are modified by oxygen impurities of a concentration ranging from 0 to 0.03. We neglect the effect of impurities on the thermodynamic parameters taking into account only their dominant effect on the London penetration depth and the GL coherence length. In the dirty limit, the GL coherence length, defined in our model as

$$\xi^2 = \frac{n \hbar^2}{m^* \gamma (T_c^2 - T^2)}, \quad (\text{A17})$$

scales with the square-root of the mean free path l , $\xi \propto \sqrt{l}$, while the effective London penetration depth scales with its inverse, $\lambda_{\text{Lon}} \propto 1/\sqrt{l}$.²⁸ Accordingly, the GL parameter $\kappa = \lambda_{\text{Lon}}/\xi$ is proportional to the inverse mean free path, $\kappa \propto 1/l$. One can see that the proper scaling of both characteristic lengths is achieved by the scaling of the effective mass,

$$m = m_0 \frac{\kappa_0}{\kappa_{\text{pure}}}, \quad (\text{A18})$$

where κ_{pure} is the GL parameter of the pure Niobium while κ_0 is the actual value for a given concentration of impurities provided in Ref. 42.

critical temperature ⁴⁵	T_c	9.5 K
Debye temperature ⁴⁵	θ_D	275 K
coupling parameter ⁴²	λ	0.89
Coulomb pseudopot. ⁴²	μ^*	0.15
coef. of spec. heat ⁴⁵	γ	719 J m ⁻³ K ⁻²
mass in pure Nb ⁴⁶	m_0	1.2 m_e
hole density ⁴⁵	n	2.2 10^{28} m^{-3}
log. der. ⁴³	$\frac{\partial \ln \mathcal{D}_0}{\partial E_F}$	1.1 10^{19} J^{-1}
GL parameter ⁴²	κ_{pure}	0.78
density of states (A1)	\mathcal{D}	5.7 $10^{47} \text{ J}^{-1} \text{ m}^{-3}$
bare density ... (A3)	\mathcal{D}_0	3.0 $10^{47} \text{ J}^{-1} \text{ m}^{-3}$
BCS interaction (A4)	V	2.9 10^{-48} J m^3
cond. energy (30)	ε_{con}	1.6 10^4 J m^{-3}
cond. en. per pair	$\frac{2\varepsilon_{\text{con}}}{n}$	9.17 10^{-6} eV
coefficient (A7)	$\frac{1}{2} \frac{\partial \gamma}{\partial n} T_c^2$	3.85 10^{-6} eV
coefficient (A15)	$\frac{\partial \varepsilon_{\text{con}}}{\partial n}$	8.73 10^{-6} eV
coefficient of C_1	$\frac{\partial \ln \varepsilon_{\text{con}}}{\partial \ln n}$	1.9
coefficient of C_2	$\frac{\partial \ln \gamma}{\partial \ln n}$	0.42

Table 1. Material parameters of pure Niobium.

¹ F. Bopp, Z. f. Phys. **107** 623 (1937).

² F. London, *Superfluids* (Wiley, New York, 1950), Vol. I, Sec. 8.

³ T. K. Hunt, Phys. Lett. **22**, 42 (1966).

⁴ J. Bok and J. Klein, Phys. Rev. Lett. **20**, 660 (1968).

⁵ J. B. Brown and T. D. Morris, Proc. 11th Int. Conf. Low Temp. Phys., Vol. 2, 768 (St. Andrews, 1968).

⁶ T. D. Morris and J. B. Brown, Physica **55**, 760 (1971).

⁷ Yu. N. Chiang and O. G. Shevchenko, Fiz. Nizk. Temp. **12**, 816 (1986) [Low. Temp. Phys. **12**, 462 (1986)].

⁸ Yu. N. Chiang and O. G. Shevchenko, Fiz. Nizk. Temp. **22**, 669 (1996) [Low. Temp. Phys. **22**, 513 (1996)].

⁹ P. Lipavský, J. Koláček, J. J. Mareš and K. Morawetz,

- cond-mat/0104192, to appear in Phys. Rev. B (December 2001).
- ¹⁰ K. I. Kumagai, K. Nozaki and Y. Matsuda, Phys. Rev. B **63**, 144502 (2001).
 - ¹¹ G. Blatter, M. Feigel'man, V. Geshkenbein, A. Larkin and A. van Otterlo, Phys. Rev. Lett. **77**, 566 (1996).
 - ¹² M. V. Feigel'man, V. B. Geshkenbein, A. I. Larkin and V. M. Vinokur, Pisma Zh. Eksp. Teor. Fiz. **62**, 811 (1995) [JETP Lett. **62**, 835 (1995)].
 - ¹³ J. Koláček and P. Lipavský, Physica C **364-365**, 138 (2001).
 - ¹⁴ A. G. van Vijfeijken and F. S. Staas, Phys. Lett. **12**, 175 (1964).
 - ¹⁵ E. Jakeman and E. R. Pike, Proc. Phys. Soc. **91**, 422 (1967).
 - ¹⁶ V. S. Sorokin, JETP **19**, 553 (1949).
 - ¹⁷ J. Bardeen, L. Cooper and J. Schrieffer, Phys. Rev. **108**, 1175 (1957).
 - ¹⁸ C. J. Gorter and H. B. G. Casimir, Phys. Z. **35**, 963 (1934).
 - ¹⁹ C. J. Gorter and H. B. G. Casimir, Z. Techn. Phys. **15**, 539 (1934).
 - ²⁰ C. J. Gorter and H. B. G. Casimir, Physica, Haag **1**, 306 (1934).
 - ²¹ J. Koláček, P. Lipavský and E. H. Brandt, Phys. Rev. Lett. **86**, 312 (2001).
 - ²² G. Rickayzen, J. Phys. C **2**, 1334 (1969).
 - ²³ C. J. Adkins and J. R. Waldram, Phys. Rev. Lett. **21**, 76 (1968).
 - ²⁴ K. M. Hong, Phys. Rev. B **12**, 1766 (1975).
 - ²⁵ J. Bardeen, *Theory of Superconductivity* in Handbuch der Physik, Bd. XV. (1955).
 - ²⁶ J. Bardeen, Phys. Rev. **94**, 554 (1954).
 - ²⁷ W. L. Ginsburg and L. D. Landau, Ž. eksper. teor. Fiz. **20**, 1064 (1950).
 - ²⁸ M. Tinkham, *Introduction to superconductivity* (McGraw-Hill, New York, 1996).
 - ²⁹ J. R. Waldram, *Superconductivity of Metals and Cuprates* (Arrowsmith, Bristol 1996).
 - ³⁰ N. R. Werthamer, *The Ginzburg-Landau Equations and Their Extensions* in *Superconductivity*, edited by R. D. Parks, page 321 (Marcel Dekker, Inc., New York, 1969).
 - ³¹ D. Ter Haar, *Elements of Hamiltonian mechanics* (North-Holland, 1961).
 - ³² J. M. Ziman, *Electrons and Phonons*, eq. (9.11.9), (Oxford University Press, London, 1960).
 - ³³ R. P. Feynman, R. B. Leighton and M. Sand, *The Feynman Lectures on Physics*, Vol. III, Sec. 21-8 (Addison-Wesley, Massachusetts, 1965).
 - ³⁴ E. H. Brandt, Phys. Rev. Lett. **78**, 2208 (1997).
 - ³⁵ M. M. Doria, J. E. Gubernatis and D. Rainer, Phys. Rev. B **39**, 9573 (1989).
 - ³⁶ U. Klein and B. Pöttinger, Phys. Rev. B **44**, 7704 (1991).
 - ³⁷ R. Ehrat and L. Rinderer, Proc. 11th Int. Conf. Low. Temp. Phys. (St-Andrews, Scotland, 1968).
 - ³⁸ R. Ehrat and L. Rinderer, Journal of Low Temp. Phys. **17**, 255 (1974).
 - ³⁹ G. Fisher and K. D. Usadel, Solid State Commun. **9**, 103 (1971).
 - ⁴⁰ A. E. Jacobs, Phys. Rev. Lett. **26**, 629 (1971).
 - ⁴¹ A. E. Jacobs, Phys. Rev. B **4**, 3022 (1971).
 - ⁴² C. C. Koch, J. O. Scarbrough and D. M. Kroeger, Phys. Rev. B **9**, 888 (1974).
 - ⁴³ N. Elyashar and D. D. Koelling, Phys. Rev. B **15**, 3620 (1977).
 - ⁴⁴ C. M. Varma and R. C. Dynes, in *Superconductivity in d- and f- band metals*, edited by D. H. Douglass (Plenum Press, New York, 1976).
 - ⁴⁵ C. Kittel, *Introduction to Solid State Physics* (Wiley, 1976).
 - ⁴⁶ L. L. Boyer, D. A. Papaconstantopoulos and B. M. Klein, Phys. Rev. B **15**, 3685 (1977).